MARTIN MARIETTA ENERGY SYSTEMS LIBRARIES

3 4456 0422645 1

ornl

ORNL/TM 12873

OAK RIDGE
NATIONAL
LABORATORY

MARTIN MARIETTA

Combining the QMR Method with First Principles Electronic Structure Codes

Noël M. Nachtigal
William A. Shelton
George M. Stocks

OAK RIDGE NATIONAL LABORATORY
CENTRAL RESEARCH LIBRARY
CIRCULATION SECTION
4500N ROOM 175
LIBRARY LOAN COPY
DO NOT TRANSFER TO ANOTHER PERSON
If you wish someone else to see this report, send in name with report and the library will arrange a loan.

MANAGED BY
MARTIN MARIETTA ENERGY SYSTEMS, INC.
FOR THE UNITED STATES
DEPARTMENT OF ENERGY

This report has been reproduced directly from the best available copy.

Available to DOE and DOE contractors from the Office of Scientific and Technical Information, P.O. Box 62, Oak Ridge, TN 37831; prices available from (615) 576-8401, FTS 626-8401.

Available to the public from the National Technical Information Service, U.S. Department of Commerce, 5285 Port Royal Rd., Springfield, VA 22161.

This report was prepared as an account of work sponsored by an agency of the United States Government. Neither the United States Government nor any agency thereof, nor any of their employees, makes any warranty, express or implied, or assumes any legal liability or responsibility for the accuracy, completeness, or usefulness of any information, apparatus, product, or process disclosed, or represents that its use would not infringe privately owned rights. Reference herein to any specific commercial product, process, or service by trade name, trademark, manufacturer, or otherwise, does not necessarily constitute or imply its endorsement, recommendation, or favoring by the United States Government or any agency thereof. The views and opinions of authors expressed herein do not necessarily state or reflect those of the United States Government or any agency thereof.

ORNL/TM-12873

Engineering Physics and Mathematics Division 405

Mathematical Sciences Section

COMBINING THE QMR METHOD WITH FIRST PRINCIPLES ELECTRONIC STRUCTURE CODES

Noël M. Nachtigal †
William A. Shelton †
George M. Stocks *

† Computing and Mathematical Sciences Division
Oak Ridge National Laboratory
Oak Ridge, TN 37831-6367
* Metals and Ceramics Division
Oak Ridge National Laboratory
Oak Ridge, TN 37831-6114

Date Published April, 1995

Research was supported by the Applied Mathematical Sciences and by the Division of Materials Sciences, Office of Energy Research, U.S. Department of Energy.

Prepared by the
Oak Ridge National Laboratory
Oak Ridge, Tennessee 37831
managed by
Martin Marietta Energy Systems, Inc.
for the
U.S. DEPARTMENT OF ENERGY
under Contract No. DE-AC05-84OR21400

MARTIN MARIETTA ENERGY SYSTEMS LIBRARIES

3 4456 0422645 1

Contents

1 Introduction 1
2 Local Density Approximation 1
3 Multiple Scattering Theory 2
3.1 Real-Space Multiple Scattering Method 6
3.2 Group-Theoretical Techniques 7
4 Results 10
5 Conclusions 12
6 References 12

COMBINING THE QMR METHOD WITH FIRST PRINCIPLES ELECTRONIC STRUCTURE CODES

Noël M. Nachtigal
William A. Shelton
George M. Stocks

Abstract

First principles methods are used to aid the metallurgist in the investigation and design of new materials. However, these methods suffer from an $\mathcal{O}(N^3)$ scaling which restricts the problem sizes that can be addressed. By incorporating the QMR method into a first principles algorithm we are able to attain $\mathcal{O}(N)$ scaling for the problem sizes of interest. This advancement will provide researchers with the necessary tools to treat large systems.

1. Introduction

The design of new technologically advanced materials is of extreme importance to the industrial and economical competitiveness of the U.S. For example, the design of a high temperature ductile intermetallic alloy could save the power generation and aerospace industries billions of dollars. The modern design of new materials makes use of local-density approximation (LDA) based, first principles electronic structure calculations. These methods are parameter-free methods, requiring no experimental input. They are predictive methods that can be used to accurately calculate materials properties. Other types of simulations that require input parameters, such as ones based on pre-defined potential functions, cannot always be used to calculate physical properties where the microscopic interactions (electronic structure) play a dominant role.

Unfortunately, current LDA based, first principles electronic structure methods exhibit $\mathcal{O}(N^3)$ scaling that renders the study of systems comprised of hundreds of atoms computationally intractable. The $\mathcal{O}(N^3)$ scaling arises due to either an eigenvalue-eigenvector computation or a matrix inversion. Our problem concerns the latter and by incorporating a quasi-minimal residual (QMR) method into our codes, we are able to achieve $\mathcal{O}(N)$ scaling for the problem sizes of interest.

The remaining sections of the paper are organized as follows, a brief description of the local density approximation will be given in section 2. In section 3, multiple-scatterng theory, the real-space method and group-theoretical techniques will be described. The results are presented in section 4 and the conclusions are given in section 5.

2. Local Density Approximation

The density functional theory (DFT) is an exact method for calculating the energetics of an electron system in the field of the atomic nuclei within a single-particle framework [8]. This theory in principle includes all collective excitations of the many-body quantum mechanical system; in particular, it includes the quantum mechanical effects of electron exchange (Pauli-exclusion principle) and correlation.

The crux of the theory is that the electron density is used as a basic variable. The total energy of the system is then expressed as a unique functional of the electron density. This functional has a unique minimum, and the electron density that yields this minimum corresponds to the correct ground-state energy. At the heart of this formalism is the calculation of a non-local, exchange-correlation potential that accounts for the many-body effects of electron exchange and correlation. However, the non-local exchange-correlation potential is unknown, requiring an approximation.

The local-density approximation to density functional theory is a technique for treating the unknown non-local exchange-correlation potential within a mean-field theoretical framework. It results in a set of single-body Schrödinger-like equations, the Kohn-Sham

equations, with an effective potential containing a local exchange-correlation potential [10]:

$$[-\nabla^2 + V^{eff}(\vec{r})]\psi_i(\vec{r}) = \epsilon_i \psi_i(\vec{r}). \tag{1}$$

Once the eigenvalues and the eigenvectors are computed, the new charge density is obtained by summing over products of an eigenvector with its complex conjugate,

$$\rho(\vec{r}) = \sum_i \psi_i(\vec{r})^* \psi_i(\vec{r}), \tag{2}$$

where the summation is performed only over the occupied electronic states. A new $V^{eff}(\vec{r})$ is obtained by solving Poisson's equation with the new charge density and, together with the eigenvalues' sum, is used to calculate the new total energy. This procedure is repeated until the difference between successive iterates of the total energy is less than a pre-defined tolerance; typically, $1.0E{-}6$ is used. At this point self-consistency has been achieved and the program terminates. There are various ways to solve the above Schrödinger-like equations and the technique used in this report is a Green's function based multiple scattering method that will be described in the following section.

It should be noted that the DFT-LDA theory is a ground-state theory. The eigenvalues of the Kohn-Sham equations represent the true eigenvalues of the system only in its ground state and are not the true eigenvalues for the excited states.

3. Multiple Scattering Theory

Multiple scattering theory is a specialization rather than a generalization of scattering theory. It can be visualized as a succession of scattering events and has the added advantage of expressing the scattering properties of the entire system in terms of the scattering properties of the individual scatterers. Its usage dates back to 1892 when Lord Rayleigh [13] first developed the theory of light scattering. Ewald [1] further developed the theory and applied it to electromagnetic waves, while Korringa, Kronig and Smit [12] used it to study acoustic waves. The focus of this article is based on the work of Korringa [11], who was the first to apply multiple scattering theory to the calculation of the electronic structure of periodic systems. It should be mentioned that at approximately the same time Kohn and Rostoker [9] arrived at the same set of equations as Korringa. However, they used a variational technique rather than multiple scattering theory. The method has since become known as the Korringa, Kohn and Rostoker (KKR) theory. The modern extension of this theory to include self-consistency, multiple atoms per unit cell, multiple-component coherent potential approximation (CPA), scalar relativity and spin polarization was carried out by Shelton and co-workers (see [14][6][7]).

The KKR method makes use of scattering theory to calculate the single-impurity scattering-path operator $\tau_{LL'}^{\alpha,ii}(\epsilon)$ that is then used to construct the single-site Green's

function:

$$G_i^\alpha(\vec{r},\vec{r},\epsilon) = \sum_{L,L'} [Z_L^\alpha(\vec{r},\epsilon)\tau_{LL'}^{\alpha,ii}(\epsilon)Z_{L'}^\alpha(\vec{r},\epsilon) - Z_L^\alpha(\vec{r},\epsilon)J_{L'}^\alpha(\vec{r},\epsilon)\delta_{LL'}], \tag{3}$$

where

i	is an atomic site;
ϵ	is the complex energy;
α	indexes the atomic species in the system;
L	refers to the angular momentum quantum numbers (ℓ, m);
$\delta_{LL'}$	is the Kronecker delta;
$Z_L^\alpha(\vec{r},\epsilon)$	is the regular single-site wave function;
$J_L^\alpha(\vec{r},\epsilon)$	is the irregular single-site wave function.

The scattering-path operator $\tau_{LL'}^{\alpha,ii}(\epsilon)$ describes the conversion of an incoming electron wave function at site i, with angular momentum index L, into an outgoing wave function at site i, with angular momentum L', while taking into account all possible scattering paths that start and end at site i. Because the system is periodic, the ith site can be assigned to any of the atomic sites in the system; we choose it to be the the origin, indexed by 0.

The general expression for $\tau_{LL'}^{ij}(\epsilon)$ is written in real-space, within an angular momentum representation, as

$$\tau_{LL'}^{ij}(\epsilon) = t_{LL'}^i(\epsilon) + t_{LL'}^i(\epsilon)\sum_{k\neq j}\sum_{L_1} G_{LL_1}^{ik}(\epsilon)\tau_{L_1L'}^{kj}(\epsilon), \tag{4}$$

where $t_{LL'}^i(\epsilon)$ is the (L, L') element of the single-site t-matrix. This depends on $V^{eff}(\vec{r})$ through the scattering phase shifts of the individual scatters, where the latter are obtained by solving the Schrödinger equation (or the Dirac equation for relativistic systems). $G_{LL'}^{ik}(\epsilon)$ is a free-electron propagator that describes how an electron is propagated from the ith site to the kth. $\tau_{LL'}^{ij}(\epsilon)$ can be formally solved in the angular momentum space, written as a matrix rather than the matrix elements, as

$$\tau^{ij} = [M^{-1}]^{ij}, \tag{5}$$

and the matrix M is written as

$$M^{ij} = [t^i]^{-1}\delta_{ij}, -G^{ij}(\vec{R}_{ij})(1-\delta_{ij}) \tag{6}$$

where $\vec{R}_{ij}$ is the distance between the ith and jth sites[2][5].

In principle, Equations (4)-(6) describe infinite-dimensional matrices labeled in the angular momentum index. For the systems under investigation, which are nearly spherically symmetric, the index L is typically truncated to a relatively small number, 2 or 3. On the other hand, for some systems, such as surfaces, which lack symmetry, or semi-conductors,

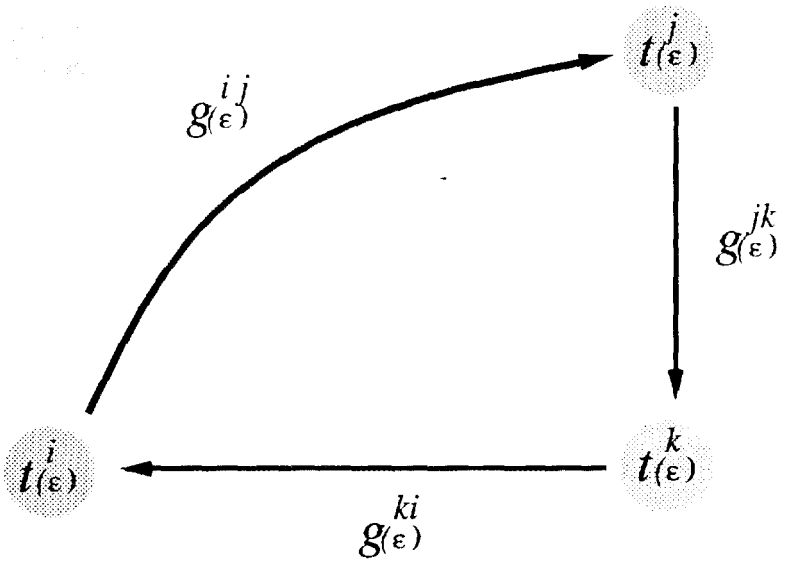

Figure 1: Schematic representation of the scattering process

which have a high degree of anisotropy, this truncation may not be justified. A schematic representation of this physical process is shown in Figure 1.

It is assumed that a crystalline solid is composed of an infinite number of atoms. Since the system is periodic, a lattice Fourier transform can be performed, resulting in

$$\tau^{00}_{LL'} = \frac{1}{\Omega_k} \int_{\Omega_k} d^3k [t^0_\ell(\epsilon)^{-1} - G_{LL'}(\vec{k}, \epsilon)]^{-1}. \tag{7}$$

This requires an explicit matrix inversion at each k point on a 3-dimensional mesh, which is the time consuming step of the calculation. The size of the matrix is $n \times (\ell + 1)^2$, where n is the number of atoms in the unit cell, and ℓ is the number of angular momentum states per atom. For example, a calculation that includes angular momentum states up to $\ell = 3$ and 13 atoms per unit cell results in a 228×228 double precision complex dense matrix. To compute the integral in (7) at a given energy ϵ requires a minimum of 300 k-points and possibly up to a couple thousand k-points. This is all performed inside a single self-consistent iteration that requires at least 32 energies per iteration to reach self-consistency and typically takes 50 iterations. A flow chart which describes the above procedure is given in Figure 2. To obtain the minimum in the total energy with respect to volume requires at least five self-consistent calculations, each at a different lattice spacing. This results in $\mathcal{O}(10^6)$ matrix inversions for one crystal structure at one concentration. Therefore, to calculate the physical properties of systems containing hundreds of atoms per unit cell demands an investigation of new techniques to invert a matrix.

The Green's function has logarithmic singularities at the eigenvalues of $\tau^{\alpha,ii}_{LL'}(\epsilon)$, which are real. To overcome this difficulty the Green's function is analytically continued into

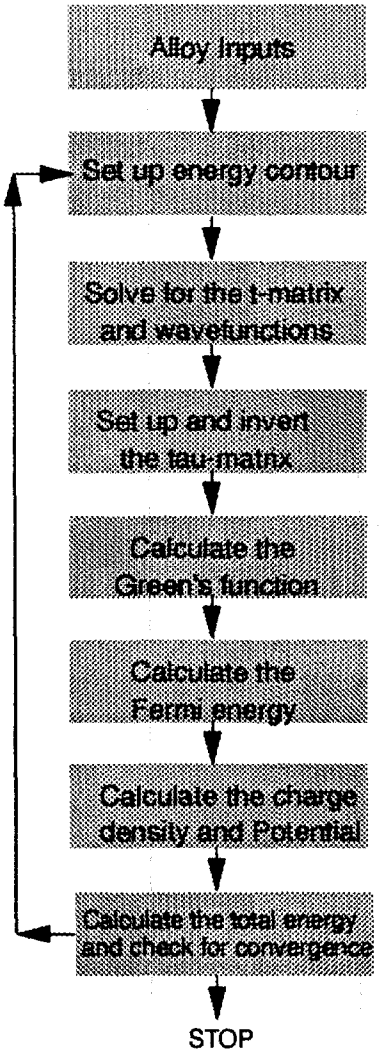

Figure 2: Flow Chart of the Real-Space Code

the complex energy plane where it has no singularities. This has the added advantage that as the imaginary part of the energy is increased, the peaks at the singularities in $\tau_{LL'}^{\alpha,00}(\epsilon)$ become very broad and thus require fewer k-points to perform the integration in (7). Therefore, the k-space mesh is set up at each energy, with the density of the mesh being determined by the imaginary part of the energy.

There are three major advantages in choosing a Green's function-based method over other band theoretical techniques. Firstly, the best method for calculating the effects of random substitutional disorder on the electronic structure is the coherent potential approximation (CPA). This method requires the Green's function. Secondly, to determine possible mechanisms responsible for some of the properties of an alloy and to calculate the transition temperature necessitates the calculation of the susceptibility, which again requires the Green's function of the system. Thirdly, there exists a natural separation between the underlying lattice structure and the potential V. This can be seen by rewriting (7) as

$$\tau_{LL'}^{00} = \frac{1}{\Omega_k} \int_{\Omega_k} d^3k [I - t_\ell^0(\epsilon) G_{LL'}(\vec{k}, \epsilon)]^{-1} t_\ell^0(\epsilon). \tag{8}$$

The term $t_\ell(\epsilon)$ is independent of the spatial coordinates and the information about the lattice structure is contained solely in $G_{LL'}(\vec{k}, \epsilon)$. As a result of this separation, the random arrangement of $t_\ell(\epsilon)$, also called the disorder, is associated with a single site only and is therefore site-diagonal. In other band theory methods there exists off-diagonal disorder that is difficult to treat in the CPA and requires further approximation.

3.1. Real-Space Multiple Scattering Method

The real-space multiple scattering method is based on multiple scattering theory. It is similar in spirit to the KKR method. However, instead of using a Fourier transform to calculate the scattering properties of the infinite system, the real-space multiple scattering method works directly in real-space; it calculates $\tau_{LL'}^{00}$ for each atom in the unit cell by including only a finite subset of atoms making up the infinite system. This results in the truncation of the summation over the site index k in (4) to a finite number of terms. At this point, instead of calculating a Fourier transform, a real-space method requires only a single inverse of a large matrix at a given energy to calculate $\tau_{LL'}^{00}$. The remaining computational steps, namely the solution of Poisson's equation and the total energy of the system, use all the atoms in the unit cell. Therefore, the only approximation occurs in the calculation of $\tau_{LL'}^{\alpha,00}(\epsilon)$, and this affects the calculation of the single-site properties, such as the electronic density of states and charge density surrounding an atom at site i, through the single-site Green's function $G_i^\alpha(\vec{r}, \vec{r}, \epsilon)$. The advantage of this method, in the context of this study, is that it is a straightforward procedure to increase the matrix size, by including more atoms in the calculation of $\tau_{LL'}^{\alpha,00}(\epsilon)$. This provides a direct procedure for testing the accuracy and robustness of the QMR method on large scale systems. In contrast, in the KKR method, the problem size cannot be increased so easily. It should be

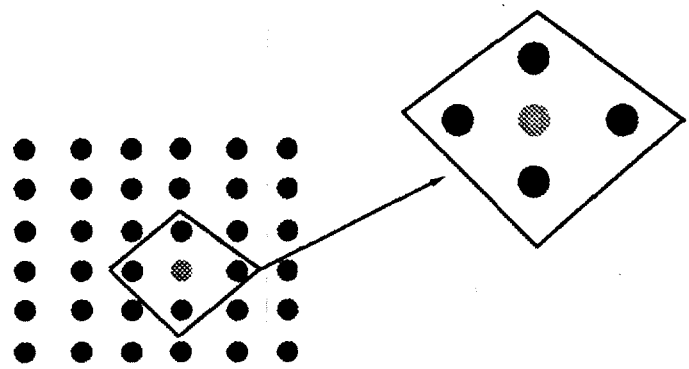

Figure 3: Schematic display of the real-space multiple scattering method. The atom at the center of the prescribed boundary calculates its scattering properties by including only those atoms that fall within the boundary. The solution to Poisson's equation and the calculation of the total energy is obtained by including all the atoms in the finite system.

noted that the results of the analysis do not depend on which code is used. The physics of the problem is the same for both codes and both codes are based on multiple scattering theory. Hence, the results of the analysis are invariant with respect to the codes.

3.2. Group-Theoretical Techniques

The application of group-theoretical techniques to solid-state physics results in the development of computationally efficient algorithms and is an effective tool for aiding in the interpretation of the results. These techniques are also extremely useful in the development process and also provide a mechanism for debugging and performance tuning. The non-zero and equal matrix elements of $\tau_{LL'}^{\alpha,00}(\epsilon)$ can be determined strictly on the basis of the symmetry of the crystal structure. In addition, the QMR method provides a natural and direct framework for implementing various types of symmetry, such as tetragonal or hexagonal, into the overall inverse algorithm.

As previously discussed, the real-space method employed here only includes a finite number of atoms to calculate the scattering properties for each atom comprising the unit cell. The number of atoms included in the calculation of $\tau_{LL'}^{\alpha,00}(\epsilon)$ is determined by a real-space cutoff distance and this procedure is used for both the periodic and aperiodic cases.

The systems dealt with in this paper are periodic, hence they are invariant to translations made up of linear combinations of the basis vectors that can be used to construct the

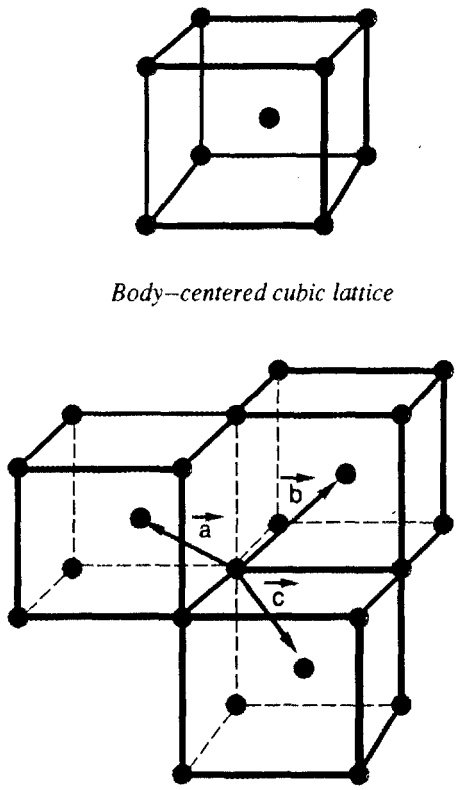

Figure 4: Schematic representation of the body-centered cubic lattice and its primitive translation vectors

crystal structure. These vectors are called the primitive translation vectors. A schematic display of the body-centered cubic (BCC) crystal structure is given in Figure 4.

Crystal structures are classified according to which space group they transform under. The space group is comprised of translation and point group operations. As seen in Figure 4, the system is invariant under certain point group operations, such as rotations or mirror reflections, and thus transforms under a particular lattice point group. The BCC crystal structure transforms under the cubic group, which means that the x, y, and z axes are equivalent, with the origin at the center of the cube. The cubic group is a sub-group of the full rotation group (spherical symmetry), and is made up of 48 point group operations. These can be easily obtained by applying all possible permutations to x, y, and z, including sign changes (reflections).

The structure of τ^{00}, such as which matrix elements are equal and non-zero, is determined by the point group it transforms under. For example, the matrix elements of the integrand in (7) can be thought of as being a tensor product of two spherical harmonics,

that is

$$\tau^{00}_{LL'}(\epsilon) = Y_L(\vec{k})\tau_{LL'}(\epsilon)Y_{L'}(\vec{k}), \tag{9}$$

where $\tau_{LL'}(\epsilon)$ is a scalar and $Y_L(\vec{k})$ is a spherical harmonic of order $L \equiv (\ell, m)$. The structure of $\tau^{00}(\epsilon)$ is found by applying the point group operators to $Y_L(\vec{k})$ and determining the group and, for a given L, the irreducible representation (Γ_i) it transforms under. For the case of complete spherical symmetry this leads to the well-known orthogonality condition for the spherical harmonics,

$$\int_{\Omega_k} d\Omega_k Y_{\ell,m}(\vec{k})Y_{\ell',m'}(\vec{k}) = \delta_{\ell,\ell'}\delta_{m,m'}, \tag{10}$$

where $Y_{\ell,m}(\vec{k})$ transforms under the mth row of the ℓth irreducible representation. For a system that has complete spherical symmetry, the number of degeneracies is equal to $2 \times \ell + 1$ and is unbounded. This reflects the fact that any infinitesimal rotation leaves the sphere invariant. However, for the cubic case there exists only a finite number of irreducible representations. For any given ℓ, the number of degeneracies cannot exceed the dimensionality of the system, which is 3 in the cubic case.

For example, consider the case where $L_{max} = 2$, so that $\ell = 0, 1, 2$. For the complete spherical case, $\tau^{00}(\epsilon)$ is 9×9, diagonal, and has 3 distinct matrix elements. There is one element for $\ell = 0$, a second that appears in triplicate for $\ell = 1$, and a third that appears five times for $\ell = 2$. For the cubic case, $\tau^{00}(\epsilon)$ is still 9×9, still diagonal, but now has 4 distinct matrix elements. There is still one element for $\ell = 0$, a second that appears in triplicate for $\ell = 1$, but for $\ell = 2$, there is a doublet and a triplet set. This is because the maximum degeneracy is limited to 3, thus forcing a lifting of the five-fold degeneracy.

A more general orthogonality condition can be written as,

$$\int_{\Omega_k} d\Omega_k Y_{\mu,\nu}(\vec{k})Y_{\mu',\nu'}(\vec{k}) = \delta_{\mu,\mu'}\delta_{\nu,\nu'}, \tag{11}$$

which is not a diagonal matrix in the angular momentum representation unless the system has complete spherical symmetry. Recall that there are only a finite number of irreducible representations for a finite group. This means that different L's will transform under the same irreducible representation, which leads to coupling between different L's and hence to off-diagonal matrix elements.

For our example above, let now $L_{max} = 3$, so that $\ell = 0, 1, 2, 3$. For the complete spherical case, $\tau^{00}(\epsilon)$ is 16×16, diagonal, and has 4 distinct matrix elements, with a fourth that appears seven times for $\ell = 3$. For the cubic case, $\tau^{00}(\epsilon)$ is still 16×16, but now it is no longer diagonal, and has 7 distinct matrix elements along the diagonal and one off-diagonal. The 9×9 leading principal submatrix remains unchanged, but for $\ell = 3$, the diagonal has two triplet sets and a singleton. In addition, there is coupling between the $\ell = 3$ spherical harmonic that transforms like x^3 and the $\ell = 1$ harmonic that transforms as x. This will introduce non-zero off-diagonal elements in the (2,13) and (13,2) positions.

Similar couplings for y and z will introduce elements in the (3,14), (4,15), (14,3), and (15,4) positions. All six off-diagonal elements are equal.

This information is used to significantly reduce the number of linear algebraic operations necessary to perform the inverse. A schematic representation of the matrix within the real-space multiple scattering method for BCC crystal with eight nearest-neighbors in its local scattering region is displayed in Figure 5. The matrix is made up of 16×16 double precision complex matrices and the upper left sub-block diagonals represent the central site in Figure 3 whose properties are to be calculated. It should be mentioned that the t-matrix associated with each row block corresponds to a particular neighboring atom. Also, it is not necessary to calculate all 16 columns of the inverse. Using the above group theoretical analysis reduces the number of columns of the inverse to be solved to 7. The first, second, fifth, eight, tenth, thirteenth and sixteenth are to be solved. The first column transforms as a constant, the second transforms as x, the third and fourth columns are equal to the second, shifted down by one and two respectively, and so on. This analysis is graphically displayed in Figure 5.

To implement the above scheme into the QMR method is straightforward. An integer array is constructed of length 16 and each element contains a non-zero entry. A `DO` loop whose range is from 1 to 16 is executed and if the corresponding integer element equals the `DO` loop index, then the QMR algorithm is performed. Otherwise, the corresponding column of the inverse is set equal to a previously calculated column, whose index is given by the integer in the array. To implement such a scheme into an LU-factorization would require considerable re-coding. Also, to add other symmetry types, such as tetragonal or hexagonal, is trivial in the QMR method but would again require a large amount of development in the LU algorithm.

4. Results

We have compared two different methods for computing the inverse of a matrix associated with perfoming electronic structure calculations on face-centered cubic (fcc) Copper and body-centered cubic (bcc) Molybdenum. The first is a direct method based on an LU-factorization and the second is the TFQMR method [3] from QMRPACK [4]. Only the leading 16 × 16 block of $\tau_{LL'}^{\alpha,00}(\epsilon)$ is required for the calculation of the single-site Green's function $G_i^{\alpha}(\vec{r},\vec{r},\epsilon)$, corresponding to the αth site. Both the LU and the TFQMR algorithms were implemented in a way that takes advantage of this. In particular, only a partial backsolve is required in LU, though the reduction in work is minor, since the full factorization is still required. For TFQMR, one needs to compute at most 16 columns. In addition, one can take advantage of the group theoretical properties discussed in the previous section, and reduce the number of columns to be solved to 7. Copper and Molybdenum were chosen because of their different physical dependencies on $\tau_{LL'}^{\alpha,00}(\epsilon)$ at the Fermi energy and the number of atoms that are necessary to accurately calculate $\tau_{LL'}^{\alpha,00}(\epsilon)$. It will be shown that these physical dependencies can have a dramatic effect on the rate

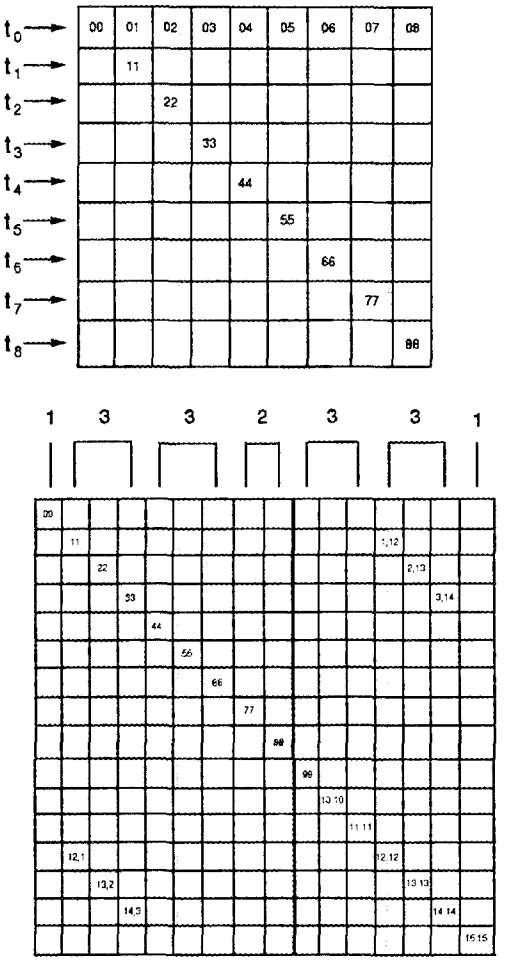

Figure 5: Schematic representation of the $\tau^{00}(\epsilon)$ and the 16×16 site-diagonal sub-block

of convergence of the TFQMR method, but that the effects are system dependent and obviously do not affect a direct method.

Figure 6 displays the time required to solve for the inverse for each energy on the contour for a specific cluster size. The time per iteration for Cu is about $0.7s$ and for Mo is about $3.5s$. All the examples shown were run on an IBM/RS6000-590 at Oak Ridge. The time rapidly increases as one approaches the Fermi energy (at the right-hand end) for both elements, but Molybdenum exhibits a substantial increase in time as compared to Copper. This is to be expected because Molybdenum has a more complex electronic structure that requires more iterations to resolve. In addition, Molybdenum requires larger cluster sizes to accurately calculate this type of behavior, along with physical properties of the system. This exemplifies the dependency of the efficiency of the TFQMR method with respect to the type of system to be investigated.

Figure 7 shows timing versus system size for the LU-based algorithm and the TFQMR method for Molybdenum. As expected, the LU-based algorithm displays cubic behavior.

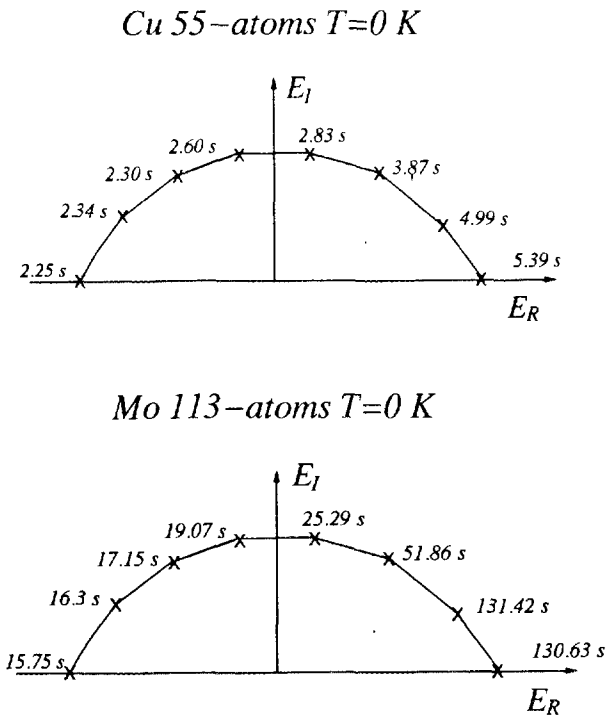

Figure 6: Time required to solve for the inverse for each energy on the contour.

However, the TFQMR method exhibits near-linear behavior in a regime where one would expect quadratic behavior (hundreds of atoms which translates into 1600×1600 double precision complex matrices). This unexpected result illustrates the robustness of the TFQMR method and as importantly, means that it may be possible to study even larger systems than was anticpiated.

5. Conclusions

The efficacious TFQMR method with its efficient use of memory makes it a highly effective algorithm that will enable material scientists to investigate large scale problems which would otherwise be untenable due to the poor N^3 scaling of direct methods. In addition, the unexpected $\mathcal{O}(N)$ scaling of the TFQMR algorithm provides researchers with the possibility of extending first principles methods to even larger systems which were previously not envisioned as being attainable.

6. References

[1] P. P. Ewald, *Zur begründung der kristalloptik*, Ann. Physik, 49 (1916), p. 117.

[2] J. S. Faulkner and G. M. Stocks, *Calculating properties with the coherent potential approximation*, Phys. Rev. B, 21 (1980), p. 3222.

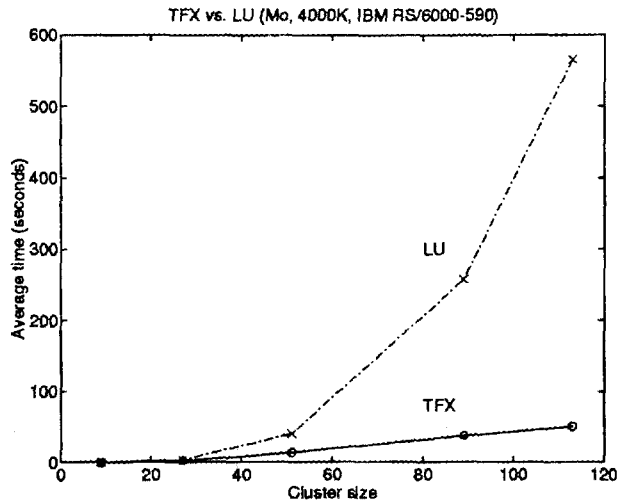

Figure 7: Comparison of timings for TFQMR vs. LU for various cluster sizes for Molybdenum

[3] R. W. FREUND, *A transpose-free quasi-minimal residual algorithm for non-Hermitian linear systems*, SIAMSci, 14 (1993), pp. 470–482.

[4] R. W. FREUND AND N. M. NACHTIGAL, *QMRPACK and applications*, Technical Report ORNL/TM–12753, Oak Ridge National Laboratory, Oak Ridge, TN, May 1994.

[5] A. GONIS, *Green functions for ordered and disordered systems*, 1992.

[6] B. L. GYORFFY, A. BARBIERI, D. D. JOHNSON, D. M. NICHOLSON, F. J. PINSKI, W. A. SHELTON, AND G. M. STOCKS, *The electronic structure and phase stabilities of metallic alloys*, in Alloy Phase Stability and Design, G. Stocks, D. P. Pope, and A. F. Giamei, eds., vol. 186, Pittsburgh, 1991, Materials Research Society, Materials Research Society, p. 3.

[7] B. L. GYORFFY, F. J. PINSKI, B. GINATEMPO, D. D. JOHNSON, J. B. STAUNTON, W. A. SHELTON, D. M. NICHOLSON, AND G. M. STOCKS, *On the causes of compositional order in the Ni_xPt_{1-x} alloys*, in Structural and Phase Stability of Alloys, J. Moran-Lopez and J. Sanchez, eds., New York, N.Y., 1992, NATO, Plenum Press, p. 167.

[8] P. HOHENBERG AND W. KOHN, *Inhomogeneous electron gas*, Phys. Rev., 136 (1964), p. 864.

[9] W. KOHN AND N. ROSTOKER, *Solution of the Schrödinger equation in periodic lattices with an application to metallic lithium*, Phys. Rev., 94 (1954), p. 1111.

[10] W. Kohn and L. J. Sham, *Self-consistent equations including exchange and correlation effects*, Phys. Rev., 140 (1965), p. 1133.

[11] J. Korringa, *On the calculation of the energy of a block wave in a metal*, Physica, 13 (1947), p. 392.

[12] J. Korringa, R. Kronig, and A. Smit, *On the theory of the reflection of sound by porous media*, Physica, 11 (1945), p. 209.

[13] L. Rayleigh, *On the influence of obstacles arranged in rectangular order upon the properties of a medium*, Phil. Mag, 23 (1892), p. 481.

[14] W. A. Shelton, *The electronic structure of the substitutionally disordered compound* $Ba_{1-x}K_xBiO_3$, 1989. PhD Thesis: University of Cincinnati (unpublished).

INTERNAL DISTRIBUTION

1. B.R. Appleton
2. T.S. Darland
3. S.L. Lee
4–8. M.R. Leuze
9–13. E.G. Ng
14. C.E. Oliver
15. B.W. Peyton
16–20. S.A. Raby
21. C.H. Romine
22–26. R.F. Sincovec
27. Central Research Library
28. ORNL Patent Office
29. K-25 Appl Tech Library
30. Y-12 Technical Library
31. Lab Records Dept - RC
32–33. Laboratory Records Dept

EXTERNAL DISTRIBUTION

34. Edward H. Barsis, Sandia National Laboratories, Computer Science and Mathematics, P.O. Box 5800, Albuquerque, NM 87185
35. Roger W. Brockett, Harvard University, 29 Oxford Street, Cambridge, MA 02138–2901
36. Oryln Edge, Illinois State University, Mathematics Department, Normal, IL 67161
37. Geoffrey C. Fox, Northeast Parallel Architectures Center, 111 College Place, Syracuse University, Syracuse, NY 13244-4100
38. J. Alan George, Vice President, Academic and Provost, Needles Hall, University of Waterloo, Waterloo, Ontario, Canada N2L 3G1
39. Gene H. Golub, Dept. of Computer Science, Stanford University, Stanford, CA 94305
40. John Gustafson, Ames Laboratory, Iowa State University, Ames, IA 50011
41. Christian Halloy, Assistant Director of JICS, 104 South College, Joint Institute for Computational Science, University of Tennessee, Knoxville, TN 37996-1301
42. Sven J. Hammarling, The Numerical Algorithms Group, Ltd., Wilkinson House, Jordan Road, Oxford OX2 8DR, United Kingdom
43. Fred Howes, Office of Scientific Computing, ER–7, Applied Mathematical Sciences, Office of Energy Research, Department of Energy, Washington, DC 20585
44. Gary Johnson, Office of Scientific Computing, ER–7, Applied Mathematical Sciences, Office of Energy Research, Department of Energy, Washington, DC 20585
45. Hans Kaper, Mathematics and Computer Science Division, Argonne National Laboratory, 9700 South Cass Avenue, Bldg. 221, Argonne, IL 60439
46. Kenneth Kennedy, Dept. of Computer Science, Rice University, P.O. Box 1892, Houston, TX 77001
47. James McGraw, Lawrence Livermore National Laboratory, P.O. Box 808, M/S L–306 Livermore, CA 94550

48. David Nelson, Director of Scientific Computing, ER–7, Applied Mathematical Sciences, Office of Energy Research, U.S. Dept. of Energy, Washington, DC 20585

49. James M. Ortega, Dept. of Applied Mathematics, Thornton Hall, University of Virginia, Charlottesville, VA 22901

50. Robert J. Plemmons, Dept. of Mathematics and Computer Science, Box 7311, Wake Forest University, Winston-Salem, NC 27109

51. James C. T. Pool, Deputy Director, Caltech Concurrent Supercomputing Facility, California Institute of Technology, Pasadena, CA 91125

52. Ahmed H. Sameh, Dept. of Computer Science, University of Minnesota, 4–192 EE/CS Bldg, 200 Union Street S.E., Minneapolis, MN 55455–0159

53. David S. Scott, Intel Scientific Computers, 15201 N.W. Greenbrier Parkway, Beaverton, OR 97006

54. Paul N. Swartztrauber, National Center for Atmospheric Research, P.O. Box 3000, Boulder, CO 80307

55. Andrew B. White, Computing Division, Los Alamos National Laboratory, P.O. Box 1663, MS-265, Los Alamos, NM 87545

56. Office of Assistant Manager for Energy Research and Development, U.S. Dept. of Energy, Oak Ridge Operations Office, P.O. Box 2001, Oak Ridge, TN 37831–8600

57–58. Office of Scientific & Technical Information, P.O. Box 62, Oak Ridge, TN 37830